Coverage Probability of Double-IRS Assisted Communication Systems

***Abstract*—In this paper, we derive the coverage probability of a double-intelligent reflecting surface (IRS) assisted wireless network and study the impact of multiplicative beamforming gain and correlated Rayleigh fading. In particular, we derive a novel closed-form expression of the coverage probability of a single-input single-output (SISO) system assisted by two large IRSs while being dependent on the corresponding arbitrary reflecting beamforming matrices (RBMs) and large-scale statistics in terms of correlation matrices. Taking advantage of th large-scale statistics, we achieve to perform optimization of the RBM of both IRSs at every several coherence intervals rather at each interval. This property, based on statistical channel state information (CSI), is of paramount importance in multi-IRS assisted networks, which are accompanied with increased computational complexity during their RBM optimization. Numerical results validate the tightness of the analytical results even for small IRSs and reveal insightful properties.**

***Index Terms*—Intelligent reflecting surface (IRS), distributed IRSs, cooperative passive beamforming, coverage probability, beyond 5G networks.**

I. Introduction

Intelligent reflecting surface (IRS) is a recent hardware technology, which promises significant increase in the energy efficiency while achieving high spectral efficiency gains. Its main advantage stems from its structure consisting of a large number of nearly passive elements that can shape the propagation environment since they can be digitally controlled by adaptively inducing amplitude changes and phase shifts on the impinging waves. As expected, these appealing advantages have attracted a lot of research interest on IRSs [1]–[5].

However, the majority of existing works have considered scenarios with one or more independently distributed IRSs subject to a single-signal reflection while not accounting for any cooperation in terms of joint passive beamforming gain over them and avoiding the undesired interference. In particular, in [6], the cooperative beamforming gain in double-IRS assisted systems with a single-antenna transmitter and receiver was shown to be of the order $\mathcal{O}(M^4)$ instead of order $\mathcal{O}(M^2)$ in single IRS systems [7], where M is the of the total IRS elements. Nevertheless, that work relied on the assumption of line-of-sight (LoS) existence for all links while only the double-reflection link between the two IRSs was considered with any other links ignored. In this direction, by assuming a multi-user multi-antenna transmitter and that both single- and double-reflection links concur. the authors in [8] and [9] maximized the minimum signal-to-interference- plus-noise ratio and proposed an efficient channel estimation scheme, respectively.

Although the study of the outage/coverage probability in IRS-assisted systems has attracted a lot of attention [10]–[14], no work has studied this metric in double-IRS assisted systems. In parallel, previous works on double-IRS assisted systems were based on the independent Rayleigh fading being unrealistic as shown in [6], [8].

With comparison to previous literature, we present the only work concerning the coverage probability for double-IRS assisted systems. Specifically, we have achieved to obtain a closed-form expression of a single-input single-output (SISO) system as the number of IRSs elements grows large. Moreover, contrary to [6], we have considered have also accounted for correlated Rayleigh fading instead of just LoS channels and we have encountered for single-reflection links to identify the realistic potentials of the proposed architecture. Furthermore, our optimization approach, based on statistical CSI, is quite advantageous in terms of computational complexity compared to [8] relying on instantaneous CSI because it can take place at every several coherence intervals instead at each coherence interval as required in instantaneous-CSI works.

Notation: Vectors and matrices are denoted by boldface lower and upper case symbols, respectively. The notations $(\cdot)^{\mathsf{T}}$, $(\cdot)^{\mathsf{H}}$, and $\mathrm{tr}(\cdot)$ represent the transpose, Hermitian transpose, and trace operators, respectively. Also, the notations $\arg(\cdot)$ and $\mod(\cdot,\cdot)$ denote the argument function and the modulus operation while the expectation operator is denoted by $\mathbb{E}[\cdot]$ and $\mathrm{diag}(\mathbf{A})$ expresses a vector with elements the diagonal elements of $\mathbf{A}$. Given two infinite sequences a_n and b_n, the relation $a_n \asymp b_n$ is equivalent to $a_n - b_n \xrightarrow[n\to\infty]{\text{a.s.}} 0$. Finally, $\mathbf{b} \sim \mathcal{CN}(\mathbf{0}, \mathbf{\Sigma})$ represents a circularly symmetric complex Gaussian vector with zero mean and covariance matrix $\mathbf{\Sigma}$.

II. System Model

We consider a double IRS cooperatively assisted communication system between a single-antenna transmitter (TX) and a single-antenna receiver (RX), where two distributed two-dimensional rectangular grid IRSs are placed in the locations of obstacles found in the intermediate space. One IRS is closer to TX, the other one is closer to the RX, and we refer to them as IRS 1 and IRS 2, respectively. Let a total of N reflecting elements with N_i denoting the number of elements of IRS i, i.e, $N_1 + N_2 = N$. Also, we address the scenario with a blocked direct signal, where RX is served through the reflection links by he IRSs. Each IRS is connected to a smart controller with the TX through a separate perfect backhaul link to adjust its phases. To focus on the properties of the double IRS assisted system, we rely on the assumption of perfect CSI. Hence, the results play the role of upper bounds of practical implementations.

Based on a block-fading model with independent channel realizations across different coherence blocks, we denote $\mathbf{g}_1 \in \mathbb{C}^{N_1\times 1}$, $\mathbf{D} \in \mathbb{C}^{N_2\times N_1}$, $\mathbf{g}_2 \in \mathbb{C}^{N_2\times 1}$, $\mathbf{u}_1 \in \mathbb{C}^{N_1\times 1}$, and $\mathbf{u}_2 \in \mathbb{C}^{N_2\times 1}$ as the channel vectors from TX to IRS 1, from IRS 1 to IRS 2, from IRS 2 to RX, from IRS 1 to RX, and from

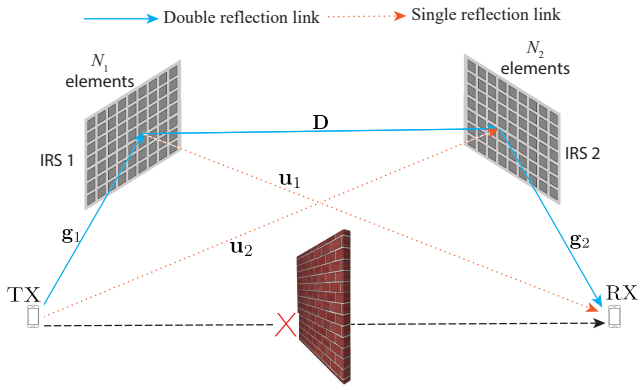

Figure 1: Double-IRS assisted model.

TX to IRS 2, respectively. Taking into account for correlated Rayleigh fading and path-loss,[1] we have

$$\mathbf{g}_1 \sim \mathcal{CN}\left(\mathbf{0}, \beta_{t1}\mathbf{R}_{t1}\right), \tag{1}$$
$$\mathbf{D} \sim \mathcal{CN}\left(\mathbf{0}, \beta_{12}\mathbf{R}_1 \otimes \mathbf{R}_2\right), \tag{2}$$
$$\mathbf{g}_2 \sim \mathcal{CN}\left(\mathbf{0}, \beta_{2r}\mathbf{R}_{2r}\right), \tag{3}$$
$$\mathbf{u}_1 \sim \mathcal{CN}\left(\mathbf{0}, \beta_{1r}\mathbf{R}_{1r}\right), \tag{4}$$
$$\mathbf{u}_2 \sim \mathcal{CN}\left(\mathbf{0}, \beta_{t2}\mathbf{R}_{t2}\right), \tag{5}$$

where β_{t1}, β_{12}, β_{2r}, β_{1r}, and β_{2r} are the path-losses while $\mathbf{R}_{t1} \in \mathbb{C}^{N\times N}$, $\mathbf{R}_1 \otimes \mathbf{R}_2 \in \mathbb{C}^{N\times N}$, $\mathbf{R}_{2r} \in \mathbb{C}^{N\times N}$, $\mathbf{R}_{1r} \in \mathbb{C}^{N\times N}$, and $\mathbf{R}_{2r} \in \mathbb{C}^{N\times N}$ are the spatial covariance matrices of the respective links. Note that the path-losses and the covariance matrices are assumed known while they can be obtained with practical methods, e.g., see [15]. Similar to [27], we assume receive RF chains integrated into the IRSs. These chains have sensing abilities and enable the acquisition of the CSI of individual channels. In particular, concerning the correlation model, we have considered a suitable model for IRSs, which is obtained under the conditions of rectangular IRSs and isotropic Rayleigh fading [16]. Specifically, let d_{V} and d_{H} denote the vertical height and horizontal width of each IRS element (both IRSs are constructed in the same way and have same size elements). Then, the (i,j)th element of the representative correlation matrix $\mathbf{R}$, $k \in \{1,2\}$ is given by

$$r_{ij} = d_{\mathrm{H}} d_{\mathrm{V}} \mathrm{sinc}\left(2\|\mathbf{u}_i - \mathbf{u}_j\|/\lambda\right), \tag{6}$$

where $\mathbf{u}_\epsilon = [0, \mod(\epsilon-1, N_{\mathrm{H}})d_{\mathrm{H}}, \lfloor(\epsilon-1)/N_{\mathrm{H}}\rfloor d_{\mathrm{V}}]^{\mathsf{T}}$, $\epsilon \in \{i,j\}$ and λ is the wavelength of the plane wave.

Relying on a slowly varying flat-fading channel model, the complex-valued received signal at the RX through the double IRS assisted network is expressed by

$$y = \left(\mathbf{g}_1^{\mathsf{H}}\mathbf{\Phi}_1\mathbf{D}\mathbf{\Phi}_2\mathbf{g}_2 + \mathbf{g}_1^{\mathsf{H}}\mathbf{\Phi}_1\mathbf{u}_2 + \mathbf{u}_1^{\mathsf{H}}\mathbf{\Phi}_2\mathbf{g}_2\right)x + n, \tag{7}$$

where $\mathbf{\Phi}_i = \mathrm{diag}\left(\alpha_{i1}\exp\left(j\theta_{i1}\right), \ldots, \alpha_{iN}\exp\left(j\theta_{iN_i}\right)\right) \in \mathbb{C}^{N_i\times N_i}$ expresses the reflecting beamforming matrix of the ith IRS, which consists of its elements with $\theta_{in} \in [0, 2\pi]$, $n = 1, \ldots, N_i$ and $\alpha_{in} \in (0,1]$ being the phase shifts and the fixed amplitude reflection coefficients of the corresponding element of the ith IRS ($i = 1,2$). The progress on loss-less meta-surfaces allows to assume maximum reflection, i.e., we set $\alpha_{in} = 1$ [3]. Moreover, x expresses the transmitted data symbol satisfying $\mathbb{E}[|x|^2] = P$ with P being the average power of the symbol, and $n \sim \mathcal{CN}(0, N_0)$ expresses the additive white Gaussian noise (AWGN) sample.

[1]The analysis could be easily extended to account for correlated Rician fading, where a LoS component exists but this is the topic of future work.

III. Coverage Probability

In this section, we present the derivation of the coverage probability when the double IRS assisted communication underlies to correlated Rayleigh fading by applying deterministic equivalent (DE) analysis tools [17].

A. Main Results

The coverage probability P_{c} is defined as the probability that the effective received SNR at the RX γ is larger than a given threshold T. Mathematically described, we have $P_{\mathrm{c}} = \Pr\left(\gamma > T\right)$, where

$$\gamma = \gamma_0 \left|\mathbf{g}_1^{\mathsf{H}}\mathbf{\Phi}_1\mathbf{D}\mathbf{\Phi}_2\mathbf{g}_2 + \mathbf{g}_1^{\mathsf{H}}\mathbf{\Phi}_1\mathbf{u}_2 + \mathbf{u}_1^{\mathsf{H}}\mathbf{\Phi}_2\mathbf{g}_2\right|^2 \tag{8}$$

is obtained based on (7) by assuming coherent communication while $\gamma_0 = P/N_0$ is the average transmit SNR. The exact derivation of this SNR is intractable while the consideration of correlated Rayleigh fading hinders further the derivation. For this reason, we resort to the DE analysis to obtain the approximated SNR, which appears to match tightly with $\Pr\left(\gamma > T\right)$ as shown in Section IV. Notably, DE tools result in tight approximations even for finite practical dimensions (see [17] and references therein). Moreover, it is worthwhile to mention that even in the single IRS assisted scenario, the majority of works on IRS-assisted systems has provided approximations based on the central limit theorem (CLT) that assumes large IRSs. Hence, similar to the existing relevant literature [10], [11], [13], we assume large IRSs ($N_i \to \infty$, $i = 1,2$).

Proposition 1: The DE SNR of a SISO transmission, enabled by a double IRS with correlated Rayleigh fading is given by

$$\frac{1}{N_1 N_2}\gamma \asymp \bar{\gamma}, \tag{9}$$

where

$$\bar{\gamma} = \gamma_0 \frac{1}{N_1 N_2}\Big(\beta_{1t}\beta_{2r}\beta_{12}\,\mathrm{tr}\left(\mathbf{R}_{1t}\mathbf{\Phi}_1\mathbf{R}_2\mathbf{\Phi}_1^{\mathsf{H}}\right)\mathrm{tr}\left(\mathbf{R}_{r2}\mathbf{\Phi}_2^{\mathsf{H}}\mathbf{R}_1\mathbf{\Phi}_2\right)$$
$$+\beta_{t1}\beta_{t2}\mathrm{tr}\left(\mathbf{R}_{t1}\mathbf{\Phi}_1\mathbf{R}_{t2}\mathbf{\Phi}_1^{\mathsf{H}}\right) + \beta_{1r}\beta_{2r}\mathrm{tr}\left(\mathbf{R}_{1r}\mathbf{\Phi}_1\mathbf{R}_{2r}\mathbf{\Phi}_1^{\mathsf{H}}\right)\Big). \tag{10}$$

Proof: See Appendix A. ∎

Obviously, the SNR in (9) depends only on the RBMs of the corresponding IRSs and the statistical CSI in terms of the path-losses and the covariance matrices of the various channels involved.

Proposition 2: The coverage probability of a SISO transmission, enabled by a double IRS with correlated Rayleigh fading for arbitrary phase shifts, is tightly approximated as

$$P_{\mathrm{c}} \approx \sum_{n=1}^{M}\binom{M}{n}(-1)^{n+1}\,\mathrm{e}^{-n\eta\frac{T}{\bar{\gamma}}}, \tag{11}$$
$$= 1 - \left(1 - \mathrm{e}^{-\frac{\eta T}{\bar{\gamma}}}\right)^M, \tag{12}$$

where $\eta = M\left(M!\right)^{-\frac{1}{M}}$ with M being the number of terms used in the calculation.

Proof: See Appendix B. ∎

B. Reflecting beamforming matrix optimization

Herein, based on the common assumption of infinite resolution phase shifters, we propose an alternating optimization algorithm for designing the cooperative reflecting beamforming solving the problem of maximum P_{c}, which is formulated as

$$\begin{aligned}(\mathcal{P}1)\ &\max_{\boldsymbol{\Phi}_1,\boldsymbol{\Phi}_2}\quad P_{\mathrm{c}}\\ &\text{s.t } |\phi_{in}|=1,\quad i=1,2 \text{ and } n=1,\ldots,N_i,\end{aligned} \tag{13}$$

where P_{c} is given by (11) or (12) and $\phi_{in}=\exp\left(j\theta_{in}\right)$.

Not only the problem $(\mathcal{P}1)$ is non-convex and it is subject to unit-modulus constraints but also a coupling between $\boldsymbol{\Phi}_1$ and $\boldsymbol{\Phi}_2$ appears in P_{c} in terms of $\bar{\gamma}$ given by (10). For this reason, we perform alternating optimization by optimizing one of the two RBMs $\boldsymbol{\Phi}_i$ while fixing the other in an iterative manner until reaching the convergence. Each optimization is achieved in terms of the projected gradient ascent until converging to a stationary point. In particular, for given $\boldsymbol{\Phi}_1$, at the lth step, we consider the vector $\mathbf{s}_{1,l}=[\phi_{11}^l,\ldots,\phi_{1N_1}^l]^{\mathsf{T}}$, which contains the phases at this step. In the next iteration, P_{c} increases until its convergence by projecting the solution onto the closest feasible point according to $\min_{|\phi_{1n}|=1,n=1,\ldots,N_1}\|\mathbf{s}_1-\tilde{\mathbf{s}}_1\|^2$ while satisfying the unit-modulus constraint with respect to ϕ_{1n}. The next iteration point is described by

$$\tilde{\mathbf{s}}_{1,l+1}=\mathbf{s}_{1,l}+\mu\mathbf{q}_{1,l}, \tag{14}$$

$$\mathbf{s}_{1,l+1}=\exp\left(j\arg\left(\tilde{\mathbf{s}}_{1,l+1}\right)\right), \tag{15}$$

where μ is the step size derived at each iteration by using the backtracking line search [18]. Also, $\mathbf{q}_{1,l}$ expresses the ascent direction at step l, i.e., $\mathbf{q}_{1,l}=\frac{\partial P_{\mathrm{c}}}{\partial \mathbf{s}_{1,l}^*}$, which is given by the following Lemma. Note that since each IRS obeys to a similar solution, we focus on IRS 1 while similar expressions hold for the optimization of IRS 2.

Lemma 1: The derivative of the coverage probability with respect to $\mathbf{s}_{1,l}^*$ is given by

$$\begin{aligned}\frac{\partial P_{\mathrm{c}}}{\partial \mathbf{s}_{1,l}^*}=&\frac{\gamma_0}{N_1N_2}\sum_{n=1}^{M}\binom{M}{n}\frac{(-1)^{n+1}\,n\eta T}{\bar{\gamma}^2\mathrm{e}^{n\eta\frac{T}{\bar{\gamma}}}}\Big(\beta_{t1}\beta_{t2}\mathrm{diag}\left(\mathbf{R}_{t1}\boldsymbol{\Phi}_1\mathbf{R}_{t2}\right)\\ &+\beta_{1t}\beta_{2r}\beta_{12}\,\mathrm{tr}(\mathbf{R}_{r2}\boldsymbol{\Phi}_2^{\mathsf{H}}\mathbf{R}_1\boldsymbol{\Phi}_2)\,\mathrm{diag}\left(\mathbf{R}_{1t}\boldsymbol{\Phi}_1\mathbf{R}_2\right)\\ &+\beta_{1r}\beta_{2r}\mathrm{diag}\left(\mathbf{R}_{1r}\boldsymbol{\Phi}_1\mathbf{R}_{2r}\right)\Big).\end{aligned} \tag{16}$$

Proof: See Appendix C. ∎

C. Baseline Scenario: Conventional Single-IRS Assisted SISO system

We assume the baseline system, where all elements $N=N_1+N_2$ are allocated in a single IRS found in the vicinity of the TX or the RX. We denote $\tilde{\mathbf{g}}_1\sim\mathcal{CN}\left(\mathbf{0},\tilde{\beta}_t\tilde{\mathbf{R}}_t\right)$ and $\tilde{\mathbf{g}}_2\sim\mathcal{CN}\left(\mathbf{0},\tilde{\beta}_r\tilde{\mathbf{R}}_r\right)$ the baseband channels of TX-IRS and IRS-RX links, respectively. Note that $\tilde{\beta}_t$, $\tilde{\beta}_r$ $\tilde{\mathbf{R}}_t\in\mathbb{C}^{N\times N}$, $\tilde{\mathbf{R}}_r\in\mathbb{C}^{N\times N}$ are the path-losses and the correlation matrices, which are assumed to be known. The corresponding RBM is described by $\tilde{\boldsymbol{\Phi}}=\mathrm{diag}\left(\tilde{a}_1\exp\left(j\tilde{\theta}_1\right),\ldots,\tilde{a}_N\exp\left(j\tilde{\theta}_N\right)\right)\in\mathbb{C}^{N\times N}$, where $\tilde{\theta}_n\in[0,2\pi],n=1,\ldots,N$ and $\tilde{\alpha}_n=1\ \forall n$ are the phase shifts and the fixed amplitude reflection coefficients of the nth IRS element.

The received SNR is written as

$$\gamma^*=\gamma_0\left|\tilde{\mathbf{g}}_1^{\mathsf{H}}\tilde{\boldsymbol{\Phi}}\tilde{\mathbf{g}}_2\right|^2 \tag{17}$$

while its DE, [17, Lem. 4], is given by

$$\frac{1}{N}\gamma^*\asymp\bar{\gamma}^* \tag{18}$$

$$=\frac{1}{N}\gamma_0\tilde{\beta}_t\tilde{\beta}_r\,\mathrm{tr}\left(\tilde{\mathbf{R}}_t\tilde{\boldsymbol{\Phi}}\tilde{\mathbf{R}}_r\tilde{\boldsymbol{\Phi}}^{\mathsf{H}}\right). \tag{19}$$

The coverage probability of the SISO channel with a single IRS P_{c}^* is given by the expression in (11) after substituting $\bar{\gamma}$ with $\bar{\gamma}^*$. This expression can be optimized by applying again the gradient ascent method as in Subsection III-B. Specifically, to apply the same algorithm for a single IRS-assisted SISO system, we require $\frac{\partial P_{\mathrm{c}}^*}{\partial \mathbf{s}_l^*}$, which is obatained as in Appendix C by

$$\frac{\partial P_{\mathrm{c}}}{\partial \mathbf{s}_l^*}=\frac{\gamma_0\tilde{\beta}_t\tilde{\beta}_r}{N_1N_2}\sum_{n=1}^{M}\binom{M}{n}\frac{(-1)^{n+1}\,n\eta T}{(\bar{\gamma}^*)^2\mathrm{e}^{n\eta\frac{T}{\bar{\gamma}^*}}}\mathrm{diag}\left(\tilde{\mathbf{R}}_t\tilde{\boldsymbol{\Phi}}_r\right). \tag{20}$$

IV. Numerical Results

We consider a three-dimensional Cartesian coordinate system, where the locations of the transmitter, receiver, IRS 1, and IRS 2 together with the directions of the IRSs follow the lines in [6] to avoid repetition and for the sake of comparison. Similarly, the distance between the transmitter and IRS 1, between IRS 1 and IRS 2, and between IRS 2 and receiver are $r_{t1}=1$ m, $r_{12}=100$ m, and $r_{2r}=15$ m. The size of each IRS element is given by $d_{\mathrm{H}}=d_{\mathrm{V}}=\lambda/8$ [16]. The spatial correlation matrix for each IRS is given by (6). Moreover, the path-loss exponents for the TX-IRS 1 and IRS 2-RX links are set as 2.2, assuming that the IRSs are close to the corresponding TX, RX with no special obstacles in the intermediate space while the path-loss exponent for the IRS 1-IRS 2 link is set as 3 by assuming a large distance. A similar exponent is assumed for the single reflection links. The carrier frequency is 3 GHz, the system bandwidth is 10 MHz, $P=43$ dbmand the noise variance is -94 dBm.

Fig. **??**.(a) illustrates the coverage probability versus the target rate for varying N_1 based on Proposition 2. Specifically, given a specific number of elements $N=200$, we vary N_1. We observe that by increasing the number of elements in IRS 1, P_{c} increases until $N_1=100$ elements and then starts increasing. In other words, we notice the least coverage when the two IRS are implemented with almost the same number of elements, which agrees with [6], [8]. Moreover, Monte-Carlo (MC) simulations almost coincide with the analytical results, which corroborates that the Alzer's inequality, the selected value of M, and the DE analysis are valid approximations. In the same figure, we show the coverage probability of the single-IRS SISO channel for $N_1=50$ and $N_1=100$ elements

under the same conditions and we observe that the double-IRS cooperative system presents better performance.

In Fig. **??**.(b), we show the coverage probability versus the target rate for different settings. First, we focus on the impact of correlation. In particular, in the case of no correlation, P_{c} is lower since the covariance matrix of the overall channel, found in the DE SNR, does not depend on the RBMS, and thus, cannot be optimized. This observation coincides with the results in [**?**] for single-IRS assisted communication. However, if the correlation increases, e.g., due to decrease of the inter-element distance, P_{c} decreases. Moreover, if random phases shifts are assumed in both IRSs, the coverage is much lower, which means that the RBM optimization definitely improves the performance. Also, we depict the performance of the single-IRS assisted scenario for the above considerations and we observe that the double-IRS architecture provides better coverage as expected.

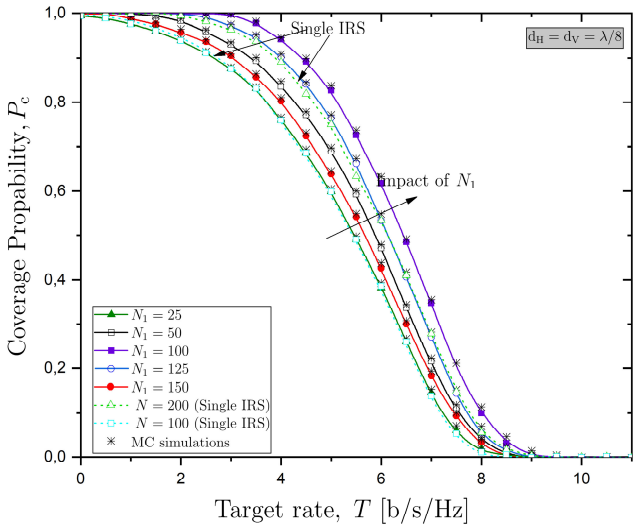

Figure 2: Coverage probability of a double-IRS assisted SISO system versus the target rate T for varying N_1 ($N = 200$, $\mathrm{d_H} = \mathrm{d_V} = \lambda/8$, analytical results and MC simulations).

V. Conclusion

In this paper, we derived the coverage probability of a double-IRS assisted SISO system under the realistic conditions of correlated Rayleigh fading. Specifically, for given RBMs, we achieved to derive its expression in closed-form in terms of large-scale statistics. Moreover, the proposed optimization over the RBMs exhibits great advantage concerning the computational complexity since it can be performed not at each coherence interval but at every several intervals. Among others, numerical results showed the outperformance of double-IRS systems over single-IRS systems and the impact of correlated Rayleigh fading. Future works on the coverage of double-IRS assisted systems could elaborate on the design of multi-user and multi-antenna transmission, and possibly, the impact of Rician fading.

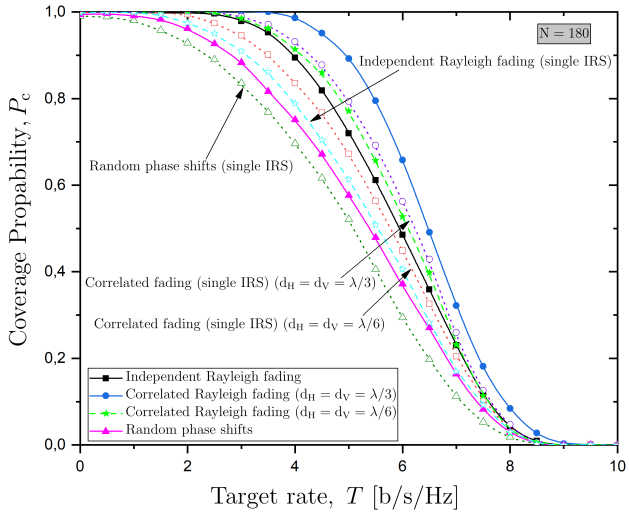

Figure 3: Coverage probability of a double-IRS assisted SISO system versus the target rate T for different correlation conditionsand with/without optimization ($N = 180$).

Appendix A
Proof of Proposition 1

The proof starts by dividing (8) with $\frac{1}{N_1 N_2}$. Hence, we have

$$\frac{1}{N_1 N_2}\gamma = \gamma_0 \frac{1}{N_1 N_2}\Bigg(\left|\mathbf{g}_1^{\mathsf{H}}\mathbf{\Phi}_1\mathbf{D}\mathbf{\Phi}_2\mathbf{g}_2\right|^2 + |\mathbf{g}_1^{\mathsf{H}}\mathbf{\Phi}_1\mathbf{u}_2|^2 + |\mathbf{u}_1^{\mathsf{H}}\mathbf{\Phi}_2\mathbf{g}_2|^2 + 2\mathrm{Re}\left((\mathbf{g}_1^{\mathsf{H}}\mathbf{\Phi}_1\mathbf{u}_2)^*\,\mathbf{g}_1^{\mathsf{H}}\mathbf{\Phi}_1\mathbf{D}\mathbf{\Phi}_1\mathbf{g}_2\right) + 2\mathrm{Re}\big((\mathbf{u}_1^{\mathsf{H}}\mathbf{\Phi}_2\mathbf{g}_2)^*\mathbf{g}_1^{\mathsf{H}}\mathbf{\Phi}_1\mathbf{D}\mathbf{\Phi}_1\mathbf{g}_2\big) + 2\mathrm{Re}\big((\mathbf{g}_1^{\mathsf{H}}\mathbf{\Phi}_1\mathbf{u}_2)^*\mathbf{u}_1^{\mathsf{H}}\mathbf{\Phi}_2\mathbf{g}_2\big)\Bigg) \tag{21}$$

$$\asymp \gamma_0 \frac{1}{N_1 N_2}\Bigg(\left|\mathbf{g}_1^{\mathsf{H}}\mathbf{\Phi}_1\mathbf{D}\mathbf{\Phi}_2\mathbf{g}_2\right|^2 + \beta_{t1}\beta_{t2}\,\mathrm{tr}\left(\mathbf{R}_{t1}\mathbf{\Phi}_1\mathbf{R}_{t2}\mathbf{\Phi}_1^{\mathsf{H}}\right) + \beta_{1r}\beta_{2r}\,\mathrm{tr}\left(\mathbf{R}_{1r}\mathbf{\Phi}_1\mathbf{R}_{2r}\mathbf{\Phi}_1^{\mathsf{H}}\right)\Bigg), \tag{22}$$

where, in (22), we have used [17, Lem. 4]. Especially, the last three terms in (21) vanish as $N \to \infty$ because of the independence between different channel vectors. The second and third terms in (22) are computed by applying [17, Lem. 4] twice. Specifically, first, we condition on $\mathbf{u}_2$ and $\mathbf{g}_2$ and apply the lemma as $N_1 \to \infty$, and then, we apply it again over $\mathbf{u}_2$ and $\mathbf{g}_2$ as $N_2 \to \infty$. Regarding the first term, we have

$$\frac{1}{N_1 N_2}\left|\mathbf{g}_1^{\mathsf{H}}\mathbf{\Phi}_1\mathbf{D}\mathbf{\Phi}_2\mathbf{g}_2\right|^2 = \frac{\beta_{1t}}{N_1 N_2}\mathrm{tr}(\mathbf{R}_{t1}\mathbf{\Phi}_1\mathbf{D}\mathbf{\Phi}_2\mathbf{g}_2\mathbf{g}_2^{\mathsf{H}}\mathbf{\Phi}_2^{\mathsf{H}}\mathbf{D}^{\mathsf{H}}\mathbf{\Phi}_1^{\mathsf{H}}) \tag{23}$$

$$= \frac{\beta_{1t}\beta_{2r}}{N_1 N_2}\,\mathrm{tr}\left(\mathbf{R}_{r2}\mathbf{\Phi}_2^{\mathsf{H}}\mathbf{D}^{\mathsf{H}}\tilde{\mathbf{R}}_{1t}\mathbf{D}\mathbf{\Phi}_2\right) \tag{24}$$

$$= \frac{\beta_{1t}\beta_{2r}\beta_{12}}{N_1 N_2}\,\mathrm{tr}\left(\mathbf{R}_{r2}\mathbf{\Phi}_2^{\mathsf{H}}\mathbf{R}_1^{1/2}\tilde{\mathbf{D}}^{\mathsf{H}}\mathbf{R}_2^{1/2}\tilde{\mathbf{R}}_{1t}\mathbf{R}_2^{1/2}\tilde{\mathbf{D}}\mathbf{R}_1^{1/2}\mathbf{\Phi}_2\right) \tag{25}$$

$$= \frac{\beta_{1t}\beta_{2r}\beta_{12}}{N_1 N_2}\,\mathrm{tr}\left(\mathbf{R}_2\tilde{\mathbf{R}}_{1t}\right)\mathrm{tr}\left(\mathbf{R}_{r2}\mathbf{\Phi}_2^{\mathsf{H}}\mathbf{R}_1\mathbf{\Phi}_2\right), \tag{26}$$

where, in 23, we have applied [17, Lem. 4] as $N_1 \to \infty$ after conditioning on $\mathbf{g}_2$ and $\mathbf{D}$. In 24, we have set $\tilde{\mathbf{R}}_{1t} =$

$\mathbf{\Phi}_1^{\mathsf{H}}\mathbf{R}_{1t}\mathbf{\Phi}_1$ and have applied [17, Lem. 4] with respect to $\mathbf{g}_2$ as $N_2 \to \infty$ conditioned on $\mathbf{D}$. In 25, we have used that $\mathbf{D} = \beta_{12}\mathbf{R}_2^{1/2}\tilde{\mathbf{D}}\mathbf{R}_1^{1/2}$ with the elements of $\tilde{\mathbf{D}}$ being of zero mean and unit variance. The last step includes application of [17, Lem. 4] with respect to $\tilde{\mathbf{D}}$, which gives $\frac{1}{N_2}\tilde{\mathbf{D}}^{\mathsf{H}}\mathbf{R}_2^{1/2}\tilde{\mathbf{R}}_{1t}\mathbf{R}_2^{1/2}\tilde{\mathbf{D}} = \frac{1}{N_2}\operatorname{tr}\left(\mathbf{R}_2\tilde{\mathbf{R}}_{1t}\right)\mathbf{I}_{N_1}$. Substitution of 26 into 22 results in the DE SNR $\bar{\gamma}$ in 10 after some simple algrebraic manipulations.

Appendix B
Proof of Proposition 2

According to the definition, the coverage probability P_{c} is basically the cumulative distribution function of the SNR. Specifically, we have

$$\mathbb{P}\left(\bar{\gamma} > T\right) \approx \tilde{\mathbb{P}}\left(\tilde{g} > \frac{T}{\bar{\gamma}}\right) \tag{27}$$

$$\approx 1 - \left(1 - \mathrm{e}^{-\eta\frac{T}{\bar{\gamma}}}\right)^M \tag{28}$$

$$= \sum_{n=1}^{M}\binom{M}{n}(-1)^{n+1}\,\mathrm{e}^{-n\eta\frac{T}{\bar{\gamma}}}, \tag{29}$$

where after substituting the DE SNR in (10) into the expression of the coverage probability, we obtain the left member of (27). In (27), we have approximated the constant number 1 by means of the dummy gamma variable $\hat{g}$, having unit mean and shape parameter M to approximate the constant number one. It has to be mentioned that this approximation becomes tighter as M goes to infinity [19], since $\lim_{y\to\infty}\frac{y^y x^{y-1}\mathrm{e}^{-yx}}{\Gamma(y)} = \delta(x-1)$ with $\delta(x)$ being Dirac's delta function. Next, in (28), we have applied Alzer's inequality (see [20]), where $\eta = M\left(M!\right)^{-\frac{1}{M}}$. In the last step, we have used the Binomial theorem.

Appendix C
Proof of Lemma 1

Application of the chain rule gives

$$\frac{\partial P_{\mathrm{c}}}{\partial \mathbf{s}_{1,l}^*} = \frac{\partial P_{\mathrm{c}}}{\partial \bar{\gamma}}\frac{\partial \bar{\gamma}}{\partial \mathbf{s}_{1,l}^*}, \tag{30}$$

where $\bar{\gamma}$ is given by (10). The first derivative in (30) is obtained as

$$\frac{\partial P_{\mathrm{c}}}{\partial \bar{\gamma}} = \sum_{n=1}^{M}\binom{M}{n}\frac{(-1)^{n+1}\,n\eta T}{\bar{\gamma}^2}\mathrm{e}^{-n\eta\frac{T}{\bar{\gamma}}}. \tag{31}$$

The derivative of $\bar{\gamma}$ with respect to $\mathbf{s}_{1,l}^*$ results in

$$\begin{aligned}\frac{\partial \bar{\gamma}}{\partial \mathbf{s}_{1,l}^*} =& \gamma_0\frac{1}{N_1N_2}\Big(\beta_{1t}\beta_{2r}\beta_{12}\operatorname{tr}(\mathbf{R}_{r2}\mathbf{\Phi}_2^{\mathsf{H}}\mathbf{R}_1\mathbf{\Phi}_2)\\ &\times\frac{\partial\left(\left(\operatorname{diag}\left(\mathbf{R}_{1t}\mathbf{\Phi}_1\mathbf{R}_2\right)\right)^{\mathsf{T}}\mathbf{s}_{1,i}^*\right)}{\partial \mathbf{s}_{1,i}^*}\\ &+\beta_{t1}\beta_{t2}\frac{\partial\left(\left(\operatorname{diag}\left(\mathbf{R}_{t1}\mathbf{\Phi}_1\mathbf{R}_{t2}\right)\right)^{\mathsf{T}}\mathbf{s}_{1,i}^*\right)}{\partial \mathbf{s}_{1,i}^*}\\ &+\beta_{1r}\beta_{2r}\frac{\partial\left(\left(\operatorname{diag}\left(\mathbf{R}_{1r}\mathbf{\Phi}_1\mathbf{R}_{2r}\right)\right)^{\mathsf{T}}\mathbf{s}_{1,i}^*\right)}{\partial \mathbf{s}_{1,i}^*}\Big)\\ =&\gamma_0\frac{1}{N_1N_2}\Big(\beta_{1t}\beta_{2r}\beta_{12}\operatorname{tr}(\mathbf{R}_{r2}\mathbf{\Phi}_2^{\mathsf{H}}\mathbf{R}_1\mathbf{\Phi}_2)\end{aligned} \tag{32}$$

$$\begin{aligned}&\times\operatorname{diag}\left(\mathbf{R}_{1t}\mathbf{\Phi}_1\mathbf{R}_2\right)+\beta_{t1}\beta_{t2}\operatorname{diag}\left(\mathbf{R}_{t1}\mathbf{\Phi}_1\mathbf{R}_{t2}\right)\\ &+\beta_{1r}\beta_{2r}\operatorname{diag}\left(\mathbf{R}_{1r}\mathbf{\Phi}_1\mathbf{R}_{2r}\right)\Big),\end{aligned} \tag{33}$$

where we have applied the property $\operatorname{tr}\left(\mathbf{A}\operatorname{diag}(\mathbf{s}_{1,l}^*)\right) = \left(\operatorname{diag}(A)\right)^{\mathsf{T}}\mathbf{s}_{1,l}^*$. Substitution of (33) and (31) into (30) provides the desired result.

References

[1] Q. Wu and R. Zhang, "Towards smart and reconfigurable environment: Intelligent reflecting surface aided wireless network," *IEEE Commun. Mag.*, vol. 58, no. 1, pp. 106–112, 2020.

[2] E. Basar *et al.*, "Wireless communications through reconfigurable intelligent surfaces," *IEEE Access*, vol. 7, pp. 116 753–116 773, 2019.

[3] E. Björnson, Ö. Özdogan, and E. G. Larsson, "Intelligent reflecting surface versus decode-and-forward: How large surfaces are needed to beat relaying?" *IEEE Wireless Commun. Lett.*, vol. 9, no. 2, pp. 244–248, 2019.

[4] A. Kammoun *et al.*, "Asymptotic max-min sinr analysis of reconfigurable intelligent surface assisted MISO systems," *IEEE Trans. Wireless Commun.*, vol. 19, no. 12, pp. 7748–7764, 2020.

[5] A. M. Elbir *et al.*, "Deep channel learning for large intelligent surfaces aided mm-Wave massive MIMO systems," *IEEE Wireless Commun. Lett.*, vol. 9, no. 9, pp. 1447–1451, 2020.

[6] Y. Han *et al.*, "Cooperative double-IRS aided communication: Beamforming design and power scaling," *IEEE Wireless Commun. Lett.*, vol. 9, no. 8, pp. 1206–1210, 2020.

[7] Q. Wu and R. Zhang, "Intelligent reflecting surface enhanced wireless network via joint active and passive beamforming," *IEEE Trans. Wireless Commun.*, vol. 18, no. 11, pp. 5394–5409, 2019.

[8] B. Zheng, C. You, and R. Zhang, "Double-IRS assisted multi-user MIMO: Cooperative passive beamforming design," *IEEE Trans. Wireless Commun.*, pp. 1–1, 2021.

[9] ——, "Efficient channel estimation for double-IRS aided multi-user MIMO system," *IEEE Trans. Commun.*, vol. 69, no. 6, pp. 3818–3832, 2021.

[10] C. Guo *et al.*, "Outage probability analysis and minimization in intelligent reflecting surface-assisted MISO systems," *IEEE Commun. Lett.*, vol. 24, no. 7, pp. 1563–1567, 2020.

[11] L. Yang *et al.*, "Coverage, probability of SNR gain, and DOR analysis of RIS-aided communication systems," *IEEE Wireless Commun. Lett.*, vol. 9, no. 8, pp. 1268–1272, 2020.

[12] T. Van Chien *et al.*, "Outage probability analysis of IRS-assisted systems under spatially correlated channels," *IEEE Wireless Commun. Lett.*, pp. 1–1, 2021.

[13] A. Papazafeiropoulos *et al.*, "Coverage probability of distributed IRS systems under spatially correlated channels," *IEEE Wireless Commun Lett.*, pp. 1–1, 2021.

[14] ——, "Intelligent reflecting surface-assisted MU-MISO systems with imperfect hardware: Channel estimation, beamforming design," *arXiv preprint arXiv:2102.05333*.

[15] D. Neumann, M. Joham, and W. Utschick, "Covariance matrix estimation in massive MIMO," *IEEE Signal Process. Lett.*, vol. 25, no. 6, pp. 863–867, 2018.

[16] E. Björnson and L. Sanguinetti, "Rayleigh fading modeling and channel hardening for reconfigurable intelligent surfaces," *IEEE Wireless Commun. Lett.*, vol. 10, no. 4, pp. 830–834, 2021.

[17] A. K. Papazafeiropoulos and T. Ratnarajah, "Deterministic equivalent performance analysis of time-varying massive MIMO systems," *IEEE Trans. Wireless Commun.*, vol. 14, no. 10, pp. 5795–5809, 2015.

[18] S. Boyd, S. P. Boyd, and L. Vandenberghe, *Convex optimization*. Cambridge university press, 2004.

[19] H. Alzer, "On some inequalities for the incomplete gamma function," *Mathematics of Computation of the American Mathematical Society*, vol. 66, no. 218, pp. 771–778, 1997.

[20] T. Bai and R. W. Heath, "Coverage and rate analysis for millimeter-wave cellular networks," *IEEE Trans. on Wireless Commun.*, vol. 14, no. 2, pp. 1100–1114, 2015.